CHARACTERIZATION OF FIBRE-DIRECTION DEPENDENT DAMPING OF GLASS-FIBRE COMPOSITES AT LOW TEMPERATURES AND LOW FREQUENCIES

Mathias Kliem[1], Jan Høgsberg[2] and Martin Dannemann[3]

[1,2] Department of Mechanical Engineering, Technical University of Denmark,
Nils Koppels Allé, 2800 Kongens Lyngby, Denmark
mkliem@mek.dtu.dk, jhg@mek.dtu.dk,
[3] Institute of Lightweight Engineering and Polymer Technology, Technische Universität Dresden,
Holbeinstrasse 3, 01307 Dresden, Germany
martin.dannemann@tu-dresden.de

Keywords: Glass-fibre composites, Damping, Loss factor, Dynamic analysis

Abstract

This paper deals with the characterization of the fibre-direction dependent damping capability of glass fibre reinforced plastics (GFRP) to be used in electrical power transmission pylons. A fibre-direction dependent damping analysis of unidirectional (UD) GFRP samples was carried out using a Dynamic Mechanical Analysis (DMA) for five different fibre orientations (0˚ | 30˚ | 45˚ | 60˚ and 90˚) and two different matrix systems (epoxy and a vinyl ester resin). Based on the dynamic characteristics the damping performance of the various composite materials was studied at three temperatures (-10˚C, 0˚C and 10˚C) and three vibration frequencies (1 Hz, 10 Hz and 30 Hz). It was observed that the loss factor of Glass Fibre Reinforced Vinyl-Ester (GF-VE) was in general slightly higher compared to the Glass Fibre Reinforced Epoxy (GF-EP). The loss factor increased slightly with temperature, while an increase in frequency led to a decrease in the damping capability of the composite material.

1 Introduction

Nonconductive composite materials such as GFRP are in the present paper considered as the structural material used for high-voltage power transmission pylons. Due to the inherent non-conductivity of the raw material components, the transmission lines could be attached directly to the cross arms of each pylon, whereby the dynamic interaction between pylon and transmission lines would be considerably increased compared to the classic design with long insulators. Wind induced vibrations and motion of the transmission lines would be transferred directly into the composite mast structure. As the self-damping capability of transmission lines is very limited [1, 2], the amplitude associated with galloping instability is a design driver for the overall architecture of large transmission line systems. By increasing the energy dissipation in the composite material, the power pylon could be made to act as a damper itself and would thereby reduce the galloping induced vibration amplitudes of the transmission lines. The material damping achieved by composite materials can be up to several orders of magnitudes higher compared to traditional engineering materials, such as steel with a loss factor between 0.00002 and 0.0003 [3, 4]. On structural level of e.g. steel lattice towers, bolts and joints have a positive impact on the structural damping, so that a loss factor of 0.04 can be achieved [5]. The damping capabilities of composite materials mainly depend on the orientation of the fibre reinforcement, the composition of the materials involved and the layup of the laminate [6]. Composite materials exhibit strong temperature- and frequency-dependent damping properties, resulting in a remarkable variation. Berthelot et al. [7] investigated the fibre-direction dependent damping of GFRP for unidirectional

Excerpt from ISBN 978-3-00-053387-7

and woven laminates, but only in the frequency range from 50 Hz to 600 Hz. In the preliminary work by Sefrani and Berthelot the effect of temperatures in the range from 20˚C to 100˚C on the fibre-direction dependent damping was studied [8]. Finally, Colakoglu analysed the natural frequency variation of flat composite beams made of woven Kevlar and polyethylene reinforcement at low and high temperatures [9]. However, a thorough investigation of the fibre-direction dependent damping at low temperatures and frequencies does not appear to have been performed, and the work of Li et al. [10], which examined the damping properties in glass fibre composites for low frequencies and temperatures, did so only in the fibre direction.

A comprehensive fibre-direction dependent damping analysis of GF-VE and GF-EP was carried out, with particular emphasis on any variations occurring at low temperatures and frequencies. The data obtained on fibre-direction dependent damping will be useful for the prediction of damping in composite structures and the subsequent design of flexible structures, such as a composite power transmission pylon, which could act as a damper to reduce the vibration amplitudes associated with transmission line galloping.

2 Analysis

2.1 Fibre-direction dependent dynamic properties

The analysis of the dynamic material properties was based on an evaluation of the response signal caused by a mechanical loading, in terms of amplitude and phase lag [11]. For a viscoelastic material, the phase lag δ between stress and strain occurs during dynamic loading, resulting in the complex elastic modulus E^*.

The separation of the complex elastic modulus into its real and imaginary part defines the storage modulus $E'(\omega)$ and the loss modulus $E''(\omega)$,

$$E^*(\omega) = E'(\omega) + jE''(\omega) \tag{1}$$

The relation between the complex modulus E^* and the storage and loss modulus $E'(\omega)$ and $E''(\omega)$ can be described in terms of the magnitude $|E^*|$ and phase lag δ by the following two relations,

$$E'(\omega) = |E^*| \cos\delta \tag{2}$$

$$E''(\omega) = |E^*| \sin\delta \tag{3}$$

The storage modulus $E'(\omega)$ represents the stiffness of a viscoelastic material and is therefore proportional to the elastically stored energy, for example during a single load cycle with vibration period $T = 2\pi/\omega$. Similarly, the loss modulus $E''(\omega)$ is proportional to the dissipation of energy during a single vibration cycle and thus represents the viscous properties of the material relative to the magnitude of its stiffness component.

The above definition of the storage and loss moduli implies that the loss factor η of a material can be determined by the following ratio between energy loss (loss modulus) and retrievable energy (storage modulus),

$$\eta = \tan\delta = \frac{E''(\omega)}{E'(\omega)} = \frac{\psi}{2\pi} \tag{4}$$

Excerpt from ISBN 978-3-00-053387-7

introducing the phase lag δ. The loss factor η is a convenient damping measure for materials because it determines the amount of energy dissipation relative to the magnitude of the stiffness component, thus giving a direct relation to the damping ratio used in the analysis of structures. The loss factor is also defined by the specific damping capacity ψ per cycle 2π.

2.2 Complex in-plane engineering constants

The full characterisation of a unidirectional (UD) laminate requires five independent material properties. This particular type of anisotropy is called transversal isotropy. As the mechanical tests take place under dynamic loading, the required material properties described by the engineering constants $E^*{}_1$, $E^*{}_2$, $G^*{}_{12}$, $G^*{}_{23}$, and $\nu^*{}_{12}$ are of a complex nature (see 2.1). The related compliance matrix can be transformed from the local fibre orientation based on the coordinate system (*1, 2, 3*) to a global coordinate system (*x, y, z*) by using a polar transformation, see Figure 1.

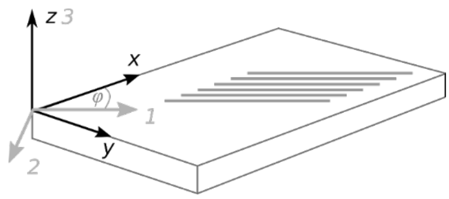

Figure 1: Local and global coordinate system of an elementary basis UD-layer (transversal isotropy).

The transformed compliance $\bar{S}_{11}$ of the first principle direction in global coordinates is described as [12]

$$\bar{S}_{11} = \frac{1}{E^*{}_\varphi} = \frac{1}{E^*{}_1}(\cos\varphi)^4 + \left(\frac{1}{G^*{}_{12}} - \frac{2\,\nu^*{}_{12}}{E^*{}_1}\right)(\sin\varphi)^2(\cos\varphi)^2 + \frac{1}{E^*{}_2}(\sin\varphi)^4 \quad (5)$$

The experimentally obtained values for the complex modulus $E^*{}_{\varphi_i.exp}$ with five different fibre directions were then used to determine the complex in-plane engineering constants $E^*{}_1$,$E^*{}_2$ and $G^*{}_{12}$ and $\nu^*{}_{12}$ of an elementary UD layer, as in (5). To minimize the error between the measured complex modulus $E^*{}_{\varphi_i.exp}$ and the calculated $E^*{}_{\varphi_i}$ the method of least squares was used in accordance to [13],

$$min \sum_{i=1}^{n}\left(E^*{}_{\varphi_i.exp} - E^*{}_{\varphi_i}(\vec{x})\right)^2 \quad with\ \vec{x} = [E^*{}_1, E^*{}_2, G^*{}_{12}, \nu^*{}_{12}]\quad and\ n \geq 4. \quad (6)$$

2.3 Fibre-direction dependent damping

The calculation of the fibre-direction dependent loss factor η for a uniaxial stress state follows the Adams-Bacon approach [14]

$$\psi_\varphi = E^*(\varphi)\left[\frac{\psi_1}{E^*{}_1}(\cos\varphi)^4 + \left(\frac{\psi_{12}}{G^*{}_{12}} - (\psi_1+\psi_2)\frac{\nu^*{}_{12}}{E^*{}_1}\right)(\sin\varphi)^2(\cos\varphi)^2 + \frac{\psi_2}{E^*{}_2}(\sin\varphi)^4\right] \quad (7)$$

where ψ_1 ,ψ_2 and ψ_{12} represent the specific damping capacity in the longitudinal, transverse and in-plane shear direction. The specific damping capacities ψ_1, ψ_2 and ψ_{12} are directly converted into the fibre-

Excerpt from ISBN 978-3-00-053387-7

direction dependent loss factors η_1, η_2 and η_{12} by (4). As in Section 2.2, the least squares method was used to minimise the error between the experimentally determined loss factors $\eta_{\varphi_i.exp}$ for the five fibre directions and the corresponding analytical values η_{φ_i},

$$min \sum_{i=1}^{n} \left(\eta_{\varphi_i.Exp} - \eta_{\varphi_i}(\vec{x}) \right)^2 \quad with\ \vec{x} = [\psi_1, \psi_2, \psi_{12}] \quad and\ n \geq 3 \tag{8}$$

3 Experimental setup

3.1 Materials

Two different matrix systems were used in the present tests: Bisphenol-Epoxy Vinyl Ester Resin (DION® IMPACT 9102-683) and an Epoxy Infusion System (PRIME™ 20LV). A technical unidirectional (UD) E-glass fabric with a total areal weight of 661 g/m^2 was also tested. While 600 g/m^2 of the reinforcing fibres were aligned in the 0˚ direction, a small portion of 50 g/m^2 were oriented in the 90˚ direction due to constraints associated with the manufacturing of the fabric. It additionally strengthens and reduces the risk of matrix failure due to loading at 90˚.

3.2 Sample preparation

A vacuum resin infusion (VaRI) process was used to fabricate UD-reinforced GFRP plates for the DMA-tests and tensile tests. Depending on the standards, different layup configurations were used to achieve the recommended thickness (t_{DMA} = 1 mm | $t_{tensile}$ = 2mm). The DMA samples and tensile test specimens were cut out by water jet in five different directions (0˚ | 30˚ | 45˚ | 60˚ and 90˚) to determine the dependence of stiffness and damping properties (loss factor) with respect to the fibre orientation.

3.3 Static and dynamic test setup

An investigation of the dynamic material properties within a certain temperature and frequency range requires a dynamic test setup. The Q800 DMA-system from TA Instruments used for the analysis can be used for measurements within a range from -150˚C to 600˚C and from 0 Hz to 200 Hz [15]. Different loading configurations can be adopted, such as bending, tension, compression and shear.

The complex modulus $E^*(\omega)$ was determined by quasi-static tensile tests using an Instron 5500R. The strain measurements were obtained by an Instron extensometer with a 50 mm gage length.

3.4 Static test procedure

The complex moduli $E^*{}_{\varphi_i,exp}$ for the two material configurations were calculated using the tensile modulus for each of the five fibre directions (0˚ | 30˚ | 45˚ | 60˚ and 90˚). The specimens with the dimensions of 250 mm x 13 mm x 3 mm were tested with general rate of deformation of 1 mm/min, which is equivalent to a quasi-static test frequency of 0.1 Hz and thus well below the dynamic range of the specimen and testing machine. The calculation of the tensile modulus was based on the ASTM standard D3039 [16]. The static test was conducted well within the elastic range of the composite material. The geometric dimensions of the specimens were measured before the static and dynamic testing. The static test conditions were carried out in climatic conditions close to the nominal values at 20˚C and 65 % relative humidity, within a range of +/- 2˚C [17].

Excerpt from ISBN 978-3-00-053387-7

3.5 Dynamic test procedure

The loss factors $\eta_{\varphi_i.exp}$ of the GF-VE and GF-EP materials were determined for combinations of three different temperatures (-10˚C, 0˚C and 10˚C), three frequencies (1 Hz, 10 Hz, and 30 Hz) and the five fibre directions (0˚ | 30˚ | 45˚ | 60˚ and 90˚). A temperature-frequency loop was defined as a sweep over the three frequencies (1 Hz, 10 Hz, and 30 Hz) for a particular temperature. The damping behaviour was then studied in the above mentioned temperature range with a cooling and heating rate of 10˚C/min to ensure a homogeneous temperature distribution within the specimen, with a rest period of 5 min at each temperature before testing. Liquid nitrogen was used to cool the specimen, and to ensure maximum deflection of the stiff composite material specimen a single cantilever clamp was used in the DMA test equipment. The specimens with the dimensions 40 mm x 10 mm x 1mm were initially clamped with 3 Nm, but after measuring three temperature-frequency loops the clamping of the samples was re-tightened to secure equal clamping conditions in all tests. To ensure optimal conditions for displacement control in the DMA the vibration amplitude was limited to 250 μm.

4 Results and Discussion

4.1 Static mechanical properties

Quasi-static tensile tests at a frequency of 0.1 Hz were used to determine the complex tensile modulus for each fibre orientation. The results are presented in Figure 2 for both composite materials.

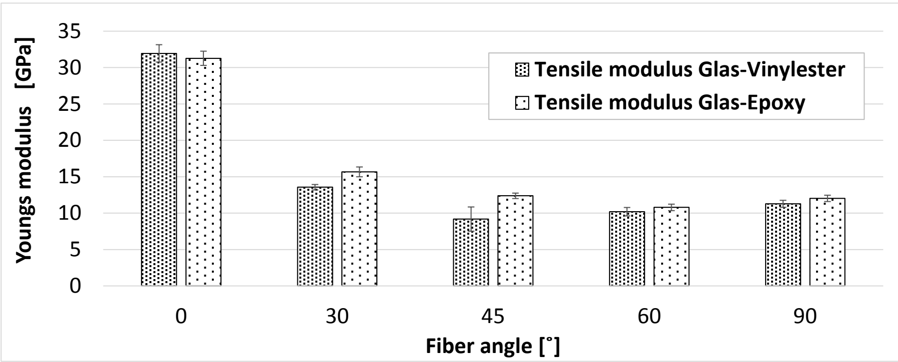

Figure 2: Direction dependent stiffness for GF-VE and GF-EP determined by tensile tests

The largest stiffness (E-modulus) was obtained at 0˚ due to the parallel-aligned fibre reinforcement. An increase in the angle-offset relative to the fibre direction (0˚) is expected to reduce the measured stiffness, due to the reduced contribution from the load-carrying fibre fabric, and this was also verified by the results. Loading at angles 30˚ | 45˚ | 60˚ and 90˚ will increasingly be carried by the matrix, whereby the apparent material stiffness is highly matrix dominated. The slight increase of the stiffness value in the transverse 90˚-direction, shown in Figure 2, is due to the previously mentioned small amount of cross fibre reinforcement that is routinely used to stabilise the main (axially oriented) fibres during commercial manufacturing.

The calculation of the complex in-plane engineering constants was carried out based on Equations (5) and (6). The results are listed in Table 1 for both composite materials: GF-EP and GF-VE.

Excerpt from ISBN 978-3-00-053387-7

Table 1: Calculated complex in-plane engineering constants for GF-EP and GF-VE

	Complex in-plane engineering constants			
Material	E^*_1 [GPa]	E^*_2 [GPa]	G^*_{12} [GPa]	ν_{12} [-]
GF-VE	31.50	10.88	3.36	0.32
GF-EP	30.42	11.56	4.05	0.28
GF-EP [18]	35.1 ± 4	9.6 ± 1	4.0 ± 0.5	0.32

The calculated material properties in Table 1 correspond well with experimental data reported in the literature [18].

The samples of GF-VE and GF-EP show similar stiffness properties for both elastic moduli $E^*_{1,2}$. As the fibre material used for the analysis was the same in all the tests, the stiffness parallel to the fibre direction (0˚) should not vary substantially. However, a slight deviation seems to occur due to different fibre-matrix adhesive characteristics, probably because two different types of resin were used in GF-VE and GF-EP. Figure 2 indicates that between angles 45˚ and 60˚ relative to the local coordinate system the stiffness reaches a minimum. The slight increase that is observed in the 60˚-direction can be explained by the small amount of additional fibre reinforcement in the transverse direction.

4.2 Dynamic mechanical properties

The fibre-direction dependent loss factor for GF-VE and GF-EP is shown in Figure 3 for all of the environmental conditions studied, based on the calculations described in 2.3.

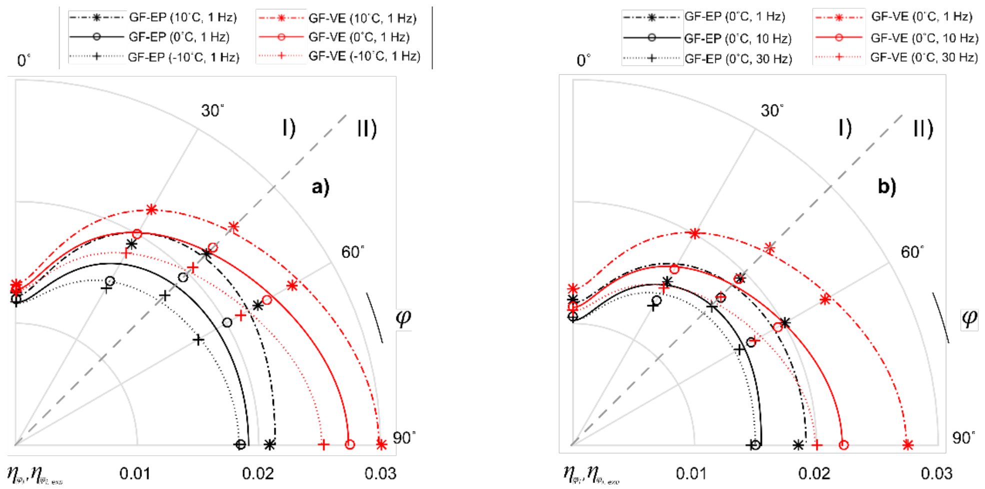

Figure 3: Loss factors η_{φ_i} and $\eta_{\varphi_i.exp}$ in dependency of a) temperature (-10˚C | 0˚C | 10˚C) and b) frequency (1 Hz | 10 Hz | 30 Hz).

As the material damping in the fibre direction (0˚) is mainly driven by fibre damping, no large variation is expected. Small differences may occur due to different adhesive characteristics. For further evaluation, the fibre-direction dependent damping plots of GF-VE and GF-EP can be subdivided into two regions based on

Excerpt from ISBN 978-3-00-053387-7

their curvature characteristics, independent of different temperatures and frequencies, see Figure 3. In the range for 0˚ < φ < 45˚ (I) the damping increases equally consistently for both materials, whereas for 45˚ < φ < 90˚ (II) substantial differences in material damping seem to occur. The damping for GF-VE gradually increases, while the material damping for GF-EP remains almost constant. The damping of GF-VE in the transverse direction (φ = 90˚) is up to 60 % higher compared to GF-EP, whereas the difference is only around 20 % for the smaller angle φ = 30˚. By inspection of the distance between adjacent curves in the polar plots, the temperature and frequency effects on the damping capacity of the composite materials accord with the results obtained for the loss modulus. The temperature-damping coupling is almost direct proportional, while the frequency-damping relation is characterized by an indirect proportionality.

5 Conclusion

In this investigation, the fibre-direction damping properties of GF-EP and GF-VE have been characterised at low temperatures and frequencies. The aim of the present study is to facilitate a preliminary design of a composite power transmission pylon, investigating whether the pylon can be used as a supplemental damper to mitigate excessive transmission line vibrations. Depending on the angle-offset relative to the fibre direction (0˚) of a UD-laminate a loss factor of 0.01 to 0.03 can be achieved on material damping level. By comparison with the literature [5], the loss factor on structural level of bolted steel lattice towers is in the range of 0.04. As composite power pylon structures are supposed to consist mainly of major, monolithic parts, additional material or structural damping, such as constrained layer damping or damping-modified resin will be required to enhance the damping in the power pylon structure to reach a sufficient damping level. However, the presented results support the following conclusions:

- The damping capacity for GF-VE was slightly higher compared to GF-EP under all the conditions studied, and was independent of the fibre direction
- The damping performance in the fibre direction was about half of the loss factor in the 45˚ and 60˚ orientations, in all three of the GFRP materials tested.
- The damping capacity increased slightly with temperature, while an increase in frequency led to a decrease in the damping capability
- The calculated dynamic mechanical properties for low frequencies and temperatures of a uniaxial stress state may be used to predict damping in composite structures with complex laminate architecture.

6 Acknowledgement

This research is supported by the Danish Government via the Innovations Foundation Denmark and the Ministry of Foreign Affairs and conducted in collaboration with Bystrup and Tuco Marine ApS, which are gratefully acknowledged. Thanks are also due to the Institute of Lightweight Engineering and Polymer Technology of TU Dresden for their kind cooperation in carrying out the experimental dynamics study of this work.

Excerpt from ISBN 978-3-00-053387-7

7 Bibliography

[1] Macdonald, J. H. G. & Larose, G. L. Two-degree-of-freedom inclined cable galloping—Part 1: General formulation and solution for perfectly tuned system. *J. Wind Eng. Ind. Aerodyn.* **96,** 291–307, 2008

[2] Macdonald, J. H. G. & Larose, G. L. Two-degree-of-freedom inclined cable galloping—Part 2: Analysis and prevention for arbitrary frequency ratio. *J. Wind Eng. Ind. Aerodyn.* **96,** 308–326, 2008

[3] Treviso, A., Van Genechten, B., Mundo, D. & Tournour, M. Damping in Composite Materials: Properties and Models. *Compos. Part B , 2015*

[4] L. Cremer and M. Heckl, Structure-Borne Sound, Springer-Verlag, New York, 1988

[5] Madugula, M.K.S., *Dynamic Response of Lattice Towers and Guyed Masts*. ASCE and American Society of Civil Engineers, 2002.

[6] Täger, O., Dannemann, M., Hufenbach, W. Analytical study of the structural-dynamics and sound radiation of anisotropic multilayered fibre-reinforced composites. *Journal of Sound and Vibration* 342:57-74, 2015

[7] Berthelot, J.-M., Assarar, M., Sefrani, Y. & Mahi, A. E. Damping analysis of composite materials and structures. *Compos. Struct.* 85:189–204, 2008

[8] Sefrani, Y. & Berthelot, J.-M. Temperature effect on the damping properties of unidirectional glass fibre composites. *Compos. Part B Eng.* 37**:** 346–355, 2006.

[9] Colakoglu, M. Effect of Temperature on Frequency and Damping Properties of Polymer Matrix Composites. *Adv. Compos. Mater.* 17:111–124, 2008.

[10] Li, J., Sun, B. & Du, Y. Damping properties of fiber reinforced composite suitable for stayed cable. *Proceedings of the Third International Conference on Smart Materials and Nanotechnology in Engineering***,** *Shenzhen, China,* 11. November 2011

[11] Ehrenstein, G. W., Riedel, G. & Trawiel, P. *Praxis der Thermischen Analyse von Kunststoffen*. Hanser Fachbuch, 2003.

[12] Berthelot, J.-M. & Sefrani, Y. Damping analysis of unidirectional glass and Kevlar fibre composites. *Compos. Sci. Technol.* 64:1261–1278, 2004.

[13] Dannemann, M. Zur vibroakustischen Auslegung von Faserverbund-Leichtbaustrukturen, Dissertation, Technische Universitaet Dresden, 2012

[14] Adams, R. D. & Bacon, D. G. C. Effect of Fibre Orientation and Laminate Geometry on the Dynamic Properties of CFRP. *J. Compos. Mater.* 7: 402–428, 1973.

[15] TA Instruments, DMA Q SeriesTM Getting Started Guide, Revision H; 2007.

[16] ASTM D3039. *Test Method for Tensile Properties of Polymer Matrix Composite Materials*. (ASTM International, 2014).

[17] DIN EN ISO 139:2011-10 - Beuth Verlag.

[18] Ghasemnejad, H. & Mirzaii, H. To Improve Mixed-Mode Interlaminar Fracture Toughness of Composite Sub-Structures. *Open J. Compos. Mater.* 04: 32–39, 2014.

Excerpt from ISBN 978-3-00-053387-7